

# Laboratory Evolution of Enantiocomplementary *Candida antarctica* Lipase B Mutants with Broad Substrate Scope

Qi Wu,<sup>†,‡</sup> Pankaj Soni,<sup>‡,§</sup> and Manfred T. Reetz<sup>\*,‡,||</sup>

<sup>†</sup>Department of Chemistry, Zhejiang University, Hangzhou, 310027, People's Republic of China

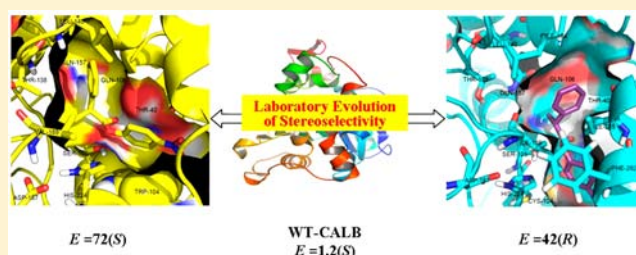
<sup>‡</sup>Max-Planck-Institut für Kohlenforschung, Kaiser-Wilhelm-Platz 1, 45470 Mülheim an der Ruhr, Germany

<sup>§</sup>CSIR-Institute of Microbial Technology, Chandigarh, 160036, India

<sup>||</sup>Fachbereich Chemie der Philipps-Universität, Hans-Meerwein-Strasse, 35032 Marburg, Germany

## S Supporting Information

**ABSTRACT:** *Candida antarctica* lipase B (CALB) is a robust and easily expressed enzyme used widely in academic and industrial laboratories with many different kinds of applications. In fine chemicals production, examples include acylating kinetic resolution of racemic secondary alcohols and amines as well as desymmetrization of prochiral diols (or the reverse hydrolytic reactions). However, in the case of hydrolytic kinetic resolution of esters or esterifying kinetic resolution of acids in which chirality resides in the carboxylic acid part of the substrate, rate and stereoselectivity are generally poor. In the present study, directed evolution based on iterative saturation mutagenesis was applied to solve the latter problem. Mutants with highly improved activity and enantioselectivity relative to wild-type CALB were evolved for the hydrolytic kinetic resolution of *p*-nitrophenyl 2-phenylpropanoate, with the selectivity factor increasing from  $E = 1.2$  (S) to  $E = 72$  (S) or reverting to  $E = 42$  (R) on an optional basis. Surprisingly, point mutations both in the acyl and alcohol pockets of CALB proved to be necessary. Some of the evolved CALB mutants are also efficient biocatalysts in the kinetic resolution of other chiral esters without performing new mutagenesis experiments. Another noteworthy result concerns the finding that enantiocomplementary CALB mutants for  $\alpha$ -substituted carboxylic acid esters also show stereocomplementarity in the hydrolytic kinetic resolution of esters derived from chiral secondary alcohols. Insight into the source of stereoselectivity was gained by molecular dynamics simulations and docking experiments.



## INTRODUCTION

Lipases (EC 3.1.1.3) catalyze the hydrolysis of carboxylic acid esters in aqueous medium but also esterification or transesterification in organic solvents.<sup>1</sup> Among the commercially available lipases that can be expressed industrially in large quantities, *Candida antarctica* lipase B (CALB; Novozyme 435) continues to be one of the most extensively used biocatalysts in both academia and industry.<sup>1,2</sup> It is robust, especially in immobilized form, and has a broad range of applications that include kinetic resolution of racemic alcohols and amines and desymmetrization of diols and diacetates as well as utility in polymer chemistry<sup>3</sup> and protection/deprotection technology.<sup>4</sup> Numerous examples pertain to the stereoselective synthesis of chiral intermediates for the production of pharmaceuticals and plant-protecting agents.<sup>1,2</sup> Dynamic kinetic resolution of alcohols and amines utilizing CALB and a racemizing transition-metal catalyst has proven to be particularly effective as pioneered by Bäckvall et al.<sup>5</sup> and Kim et al.<sup>6</sup> Moreover, a number of fascinating cases of enzyme promiscuity employing this lipase have been reported by Berglund, Hult, and others, including aldol reactions, Michael additions, vinyl polymerization, and even oxidations.<sup>7</sup>

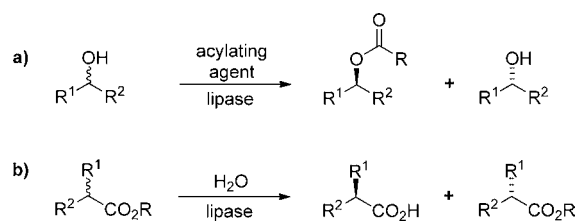
Structurally, CALB belongs to the  $\alpha/\beta$ -hydrolase family and follows the same reaction mechanism as other serine hydrolases.<sup>1</sup> The active site is characterized by the catalytic triad Ser-His-Asp, an oxyanion hole that stabilizes the transition state of the reaction, and a binding pocket composed of two domains, one for the acyl moiety of the ester and another one for the alcohol part, respectively.<sup>8</sup> Consequently, when chirality is in the alcohol part of an ester, researchers have focused on the alcohol pocket of CALB (or of any other lipase) for interpreting enantioselectivity or manipulating it by protein engineering. Kazlauskas's rule regarding the kinetic resolution of racemic secondary alcohols has served as a useful guide in the prediction of stereoselectivity.<sup>9</sup> Indeed, this transformation is one of the most important applications of CALB. When the stereogenic center belongs to the acid moiety, attention is traditionally paid to the acyl pocket of lipases.<sup>1,2</sup>

In contrast to the broad spectrum of chiral alcohols (Scheme 1a), diols, and amines accepted by CALB often with high enantioselectivity, only a limited number of substrates

Received: October 23, 2012

Published: January 9, 2013

**Scheme 1. CALB-Catalyzed Kinetic Resolution of (a) Chiral Alcohols and of (b) Chiral Esters**



containing structurally different acids or esters react at reasonable rates and acceptable stereoselectivity (Scheme 1b).<sup>1,2</sup> CALB can convert straight chain fatty acid esters of different length rapidly only when the chain length varies between C5 and C12.<sup>10</sup> The substrate scope of CALB toward sterically demanding chiral  $\alpha$ -substituted carboxylic acid esters is narrow, with low activity and poor stereoselectivity generally being observed.<sup>1,2,11</sup> For example, 2-arylpropionic acid esters of the ibuprofen-type, which are of interest as pain relievers in the pharmaceutical industry,<sup>12</sup> prove to be poor substrates, reacting slowly (or not at all) with low degrees of stereoselectivity.<sup>1,8c,10,11</sup> Some of these problems can be solved by using the analogous N-acylazoles in combination with CALB, but this requires additional synthetic steps.<sup>11c</sup> It is interesting to note that enzyme-free systems using chiral organocatalysts have been developed only recently for performing esterifying kinetic resolution of chiral acids as reported by Shiina et al.<sup>13a</sup> and Birman et al.<sup>13b</sup>

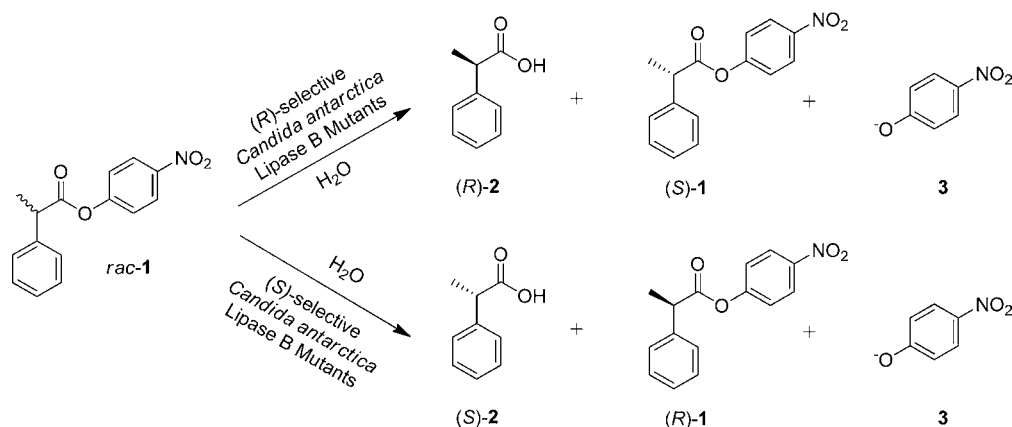
In order to further improve thermostability, activity, stereoselectivity, and expression rate of CALB and to tailor it for different applications, a range of mutants have been developed using rational design or directed evolution with notable degrees of success, generally focusing on kinetic resolution of chiral alcohols.<sup>1,14–17</sup> For example, error-prone polymerase chain reaction (PCR) applied to CALB provided mutants with >20-fold improvement in half-life at 70 °C relative to the wild type (WT).<sup>14b</sup> In the quest to increase the hydrolysis activity, circular permutation was elegantly used to produce a CALB variant with an up to 175-fold enhanced  $k_{cat}/K_M$  value over WT CALB.<sup>15a–c</sup> Various mutants such as V190A,<sup>15d</sup> L278A/W104F,<sup>15e</sup> and S47L<sup>15f</sup> were designed to improve the rate of transesterification in nonaqueous medium. Random mutagenesis at single residues or multiple positions can effectively improve the expression yield of CALB in *Escherichia coli*, *Pichia pastoris*, and *Hansenula polymorpha*.<sup>16</sup> In order to increase the stereoselectivity of CALB toward certain secondary alcohols, Hult and co-workers resorted to rational design utilizing site-specific mutagenesis in the generation of mutations S47A,<sup>17a</sup> T42V, and T40A<sup>17</sup> situated next to the alcohol binding pocket, which dramatically improved the enantioselectivity toward pentane-2-ol or halohydrins. Similarly, they discovered that the W104A mutant is able to accommodate much larger groups than WT CALB. Interestingly, this change transformed the highly *R*-selective WT into an *S*-selective mutant.<sup>17c,d</sup> Two recent studies of variant W104A describe its use in *S*-selective kinetic resolution and dynamic kinetic resolution of 1-phenylalkanols with an alkyl chain of up to eight carbon atoms, with the *S*-enantiomer being preferred.<sup>17e,f</sup> Moreover, when introducing single point mutations I189A, L278V, and A282L, which can modify the width and shape of the hydrophobic tunnel leading to the active site, significant modification of enantioselectivity was observ-

ed.<sup>17g</sup> Svendsen has written an informative review covering protein engineering of CALB and other lipases for the period up to the year 2000.<sup>17h</sup>

Given the robustness and efficient expression of CALB (tons are produced each year), it is surprising that few attempts to apply protein engineering for solving these problems have been reported to date. Brask and co-workers described the replacement of helix  $\alpha 5$  of CALB by the corresponding lid region from the CALB homologues from *Neurospora crassa* and *Gibberella zeae*, which resulted in two new CALB mutants with increased enantioselectivity in the hydrolysis of racemic ethyl 2-phenylpropanoate as measured by the selectivity factor ( $E = 50$ ), although the absolute configuration was not determined.<sup>18</sup> Lutz and co-workers reported a 2-fold increase in the  $E$  value in the esterification of 2-phenylpropanoic acid as a result of applying circular permutation.<sup>15a</sup> Relevant is also a recent study by Bäckvall and co-workers, who reported the CAST-based directed evolution of the related *C. antarctica* lipase A (CALA) resulting in the acceptance of 2-phenylpropionic acid esters and similar substrates with high *R*-selectivity; the structurally related and medicinally important ibuprofen-ester was not accepted by the mutants nor was reversal of enantioselectivity in favor of *S*-products reported.<sup>19a</sup> Fortunately, in subsequent attempts utilizing a more effective strategy based on saturation mutagenesis at multiple-residue sites, *R*-selective mutants were evolved that accept ibuprofen-type esters.<sup>19b</sup>

We reasoned that if CALB could be tuned to accept 2-arylpropionic acid esters and similar bulky esters with acceptable rates and high *R*- and *S*-enantioselectivity on an optional basis, then the range of applications of this industrially viable lipase would be broadened considerably.

Directed evolution<sup>20</sup> of stereoselective enzymes<sup>21</sup> as catalysts for asymmetric transformations in synthetic organic chemistry and/or biotechnology is now well established. Nevertheless, some uncertainty still exists as to the optimal method and strategy for probing protein sequence space optimally. Any one of the known gene mutagenesis methods such as error-prone polymerase chain reaction (epPCR), saturation mutagenesis, or DNA shuffling can be expected to provide mutants with enhanced stereoselectivity, with the degree of improvement depending upon the amount of laboratory work that the experimenter is willing to invest.<sup>20,21</sup> Since the bottleneck of directed evolution is the screening step, higher-quality and therefore smaller libraries are needed. Our contribution in this endeavor is iterative saturation mutagenesis (ISM) in its two structure-based embodiments, namely, the combinatorial active-site saturation test (CAST),<sup>21</sup> which can be applied to control stereo- and or regioselectivity, to enhance rate and to expand substrate scope of enzymes, and B-FIT for increasing the stability of proteins.<sup>22</sup> When applying iterative CASTing, appropriate sites next to or near the binding pocket of an enzyme, each comprising one or more amino acid positions, are first subjected to saturation mutagenesis with formation of focused libraries. The genes of the hits are then utilized as templates for performing saturation mutagenesis at the respective other sites, with the process being repeated until the desired degree of catalyst improvement has been achieved. This strategy relies on data from structural biology and is quite different from the more conventional approach in which point mutations originating from two or more libraries are simply combined.<sup>20,21</sup> In contrast to the latter, ISM maximizes the probability of cooperative effects acting between sets of mutations at each branching point in an upward climb and

Scheme 2. Stereoselective Hydrolysis of *rac*-1 Catalyzed by *R*- and *S*-Selective CALB Mutants

between point mutations within a set.<sup>21</sup> In order to beat the numbers problem in directed evolution further, the use of reduced amino acid alphabets as defined by appropriate codon degeneracies has proven to be a valuable tool because it cuts oversampling drastically.<sup>21</sup>

In the present study, we wanted to test the ISM approach in an attempt to evolve active and stereoselective CALB mutants suitable for the hydrolytic kinetic resolution of chiral  $\alpha$ -substituted carboxylic acid esters, while keeping the screening effort as low as possible. Obtaining both *R*- and *S*-selective CALB mutants was also part of the goal, which has not been achieved prior to this investigation.

## RESULTS AND DISCUSSION

**Experimental Platform.** The hydrolytic kinetic resolution of racemic 2-phenylpropionic acid *p*-nitrophenyl ester (*rac*-1) was chosen as the model reaction (Scheme 2), with a UV/visible plate reader monitoring the appearance of *p*-nitrophenolate (3) as a function of time.<sup>23</sup> In order to detect hits with enhanced or inverted enantioselectivity, separately synthesized (*R*)- and (*S*)-1 were used pairwise on 96-well microtiter plates, with the relative slopes of initially observed rates indicating the degree of stereoselectivity. In order to obtain reliable selectivity factors *E*, the hits were subsequently isolated and tested as catalysts in the reaction of *rac*-1. WT CALB is a poor catalyst in this reaction, as the substrate reacts sluggishly with very slight preference for (*S*)-2 (*E* = 1.2).

In order to choose appropriate sites for saturation mutagenesis, we were guided by the X-ray structure of CALB (PDB code 1TCA).<sup>8</sup> As pointed out in the Introduction, all lipases are traditionally considered to have two binding domains for harboring esters: one for the acid (acyl) part and the other for the alcohol part of the ester. Catalytically active serine as part of the triad Asp187-His224-Ser105 lies between them (Figure 1a). The structure of the acyl binding site can be subdivided into a hydrophilic region and a hydrophobic region, the so-called hydrophobic crevice. The hydrophobic crevice is defined by residues A141, L144, V149, and I285 that are located at the top of the binding site. The hydrophilic region of the binding site is characterized by residues D134, T138, and Q157. Residues A281, A282, and I285 point toward the alcohol moiety of the substrate and limit the size of the channel. The alcohol binding pocket is defined by the mainly hydrophobic residues W104, L278, A281, A282, and I285. Initially, we focused saturation mutagenesis only on sites in the acyl binding domain (sites B, C, and E as shown in Figure 1b), but as the investigation

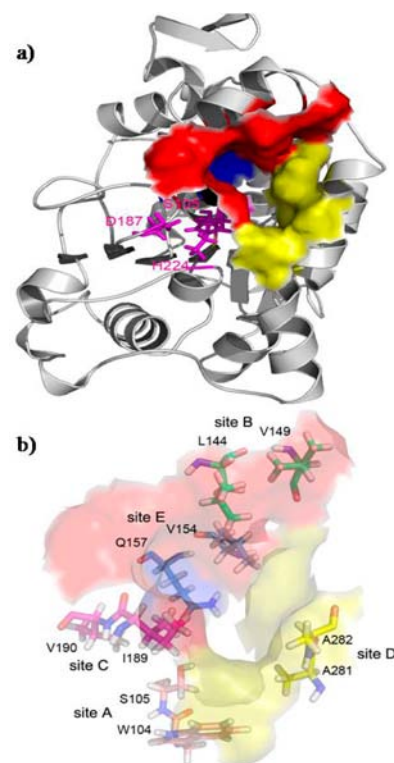


**Figure 1.** X-ray structure of WT CALB (PDB: 1TCA)<sup>8</sup> used as a guide in directed evolution. (a) The catalytic triad S105-H224-D187 is shown as purple sticks, the alcohol binding pocket as a yellow surface, and the acid binding pocket as a combination of a blue surface (hydrophilic region) and a red surface (hydrophobic region). (b) Proposed CAST sites A (W104/S105), B (L144/V149), C (I189/V190), D (A281/A282), and E (V154/Q157).

proceeded, residues in the alcohol binding pocket were also considered (sites A and D).

The 10 residues at sites A–E can in principle be treated separately as single residue sites that would call for 10 initial saturation mutagenesis experiments. Although such a strategy can be successful as shown in other studies,<sup>21</sup> we decided to group them into five two-residue sites, because this maximizes the possibility of cooperative epistatic effects within a site and between sets of mutations as the evolutionary ISM process proceeds.<sup>20n,21</sup> When choosing NNK codon degeneracy encoding all 20 canonical amino acids, saturation mutagenesis at a two-residue site requires the screening of about 3000



transformants for 95% coverage (assuming the absence of amino acid bias).<sup>21</sup> The total initial screening effort in the present case would amount to about 15 000 measurements. In order to reduce this work, we chose a reduced amino acid alphabet by turning to NDT codon degeneracy that encodes 12 amino acids (Phe, Leu, Ile, Val, Tyr, His, Asn, Asp, Cys, Arg, Ser, and Gly) and requires the screening of only 430 transformants for 95% library coverage.<sup>21</sup>

**Initial Libraries Generated by Saturation Mutagenesis.** In exploratory mutagenesis experiments at positions lining the acyl binding pocket, namely, sites B (Leu144/Val149), C (Ile189/Val190), and E (Val154/Gln157) (Figure 1b), we were surprised to discover that these libraries failed to contain notably improved variants. Although in ISM it is possible to continue upward climbs even if a library does not harbor improved variants simply by choosing nonimproved or even inferior mutants,<sup>24</sup> we decided to extend the search in protein sequence space by including sites lining the alcohol binding pocket, specifically A (Trp104/Ser105) and D (Ala281/Ala282) (Figure 1b). Note that Ser105 is part of the catalytic triad, which means that normally it would not be included in a randomization site. Nevertheless, we were curious to see if amino acid substitutions such as threonine would improve catalyst performance.

Following the generation and screening of the libraries resulting from randomization at sites A and D at the alcohol binding pocket, mutants were identified showing somewhat improved activity and enantioselectivity in the model reaction (Table 1). For example, variant SG101 (A281G/A282V) with

**Table 1. Improved First Generation CALB Mutants Obtained by Saturation Mutagenesis at Sites A and D Aligning the Alcohol Binding Pocket, with NDT Codon Degeneracy Being Employed**

mutant	reaction time (h)	conversion (%)	ee <sub>r</sub> (%)	E (R)	E (S)	sequence
RG101	6.5	29	62	5		W104C
RG102	6.5	28	39	3		W104I
WT	20	41	11		1.2	WT
SG101	1	45	57		6	A281G/A282V
SG102	1	42	19		1.6	A281G

enhanced *S*-selectivity ( $E = 6$ ) was found in library D, and two mutants displaying reversed enantioselectivity in favor of (*R*)-2 occurred in library A. Interestingly, the genetic code of Ser105 in these two mutants was changed from TCC to AGT, but the amino acid is still serine, which is the essential amino acid in the catalytic triad. Rather than repeating saturation mutagenesis at sites B, C, and E using traditional NNK codon degeneracy that would ensure a complete amino acid alphabet of 20 canonical members and therefore entail higher structural diversity, we decided to use the best *R*- and *S*-selective mutants (RG101 and SG101, respectively) as templates for saturation mutagenesis at the other sites.

**Iterative Rounds of Saturation Mutagenesis.** When considering an ISM system consisting of five sites, 120 different pathways are theoretically possible.<sup>21</sup> Rather than embarking on a systematic exploration of all pathways,<sup>24</sup> the goal of the present study was to see how far one can get by restricting the number of options severely but still achieving good *R*- and *S*-selectivity in separate pathways. Therefore, the decision was made to continue the evolutionary process along two arbitrarily

chosen routes: one directed toward *R*-selectivity and the other toward *S*-selectivity. Attention was first paid to enhancing the reversal of enantioselectivity in favor of (*R*)-2 by utilizing the gene of variant RG101 as a template for saturation mutagenesis at site D, which is likewise at the alcohol binding pocket. Three mutants with moderate *R*-selectivity were identified, namely, RG201, RG202, and RG204, with  $E$  values in the range 11–15 (Figure 2 and Table 2). The two best mutants were then used

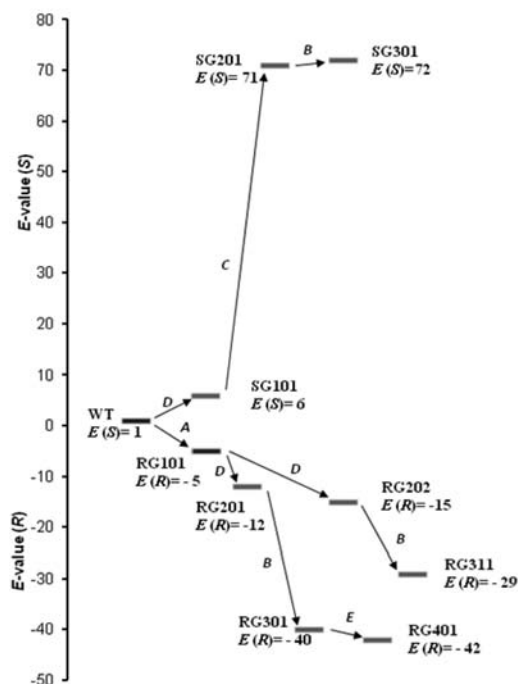


**Figure 2.** Iterative CASTing in the evolution of *R*- and *S*-enantioselective CALB mutants as catalysts in the hydrolytic kinetic resolution of *rac*-1.

to perform saturation mutagenesis at site B next to the acyl binding pocket; this ISM-branch provided notably improved variants RG311 ( $E = 29$ ) and RG301 ( $E = 40$ ) (Figure 2 and Table 2). Only one of the pathways was continued, namely, A → D → B → E, which provided variant RG401 ( $E = 42$ ). In the case of *S*-selectivity, a likewise limited number of mutagenesis experiments were performed, and the short pathway D → C → B resulted in the best variant SG301 with  $E = 72$  (Figure 2 and Table 3). An attempt to continue on this pathway by considering site E failed to induce further improvement. The total screening effort involved the evaluation of less than 10 000 transformants, which is a good score considering the fact that two different catalysts of opposite enantioselectivity were evolved. Upscaling the model reaction of *rac*-1 (40 mg) catalyzed by mutant SG301 also proved to be successful (Supporting Information).

**Substrate Scope of *S*- and *R*-Selective CALB Mutants.** Although no (bio)catalyst can ever be “universal”, organic chemists seek to develop catalysts that function well for a range of different substrates. Therefore, without performing any more mutagenesis experiments, we tested some of the best *R*- and *S*-selective CALB mutants evolved for the model substrate *rac*-1 as catalysts in the hydrolytic kinetic resolution of other racemic esters 4–13 (Table 4). Upon employing the best mutants SG301 and RG401, remarkably enhanced activity and selectivity relative to WT CALB were observed in many cases

**Table 2. Second, Third, and Fourth Generation R-Selective CALB Mutants as Catalysts in the Hydrolytic Kinetic Resolution of *rac*-1**

mutant	reaction time (h)	conversion (%)	ee <sub>R</sub> (%)	<i>E</i> ( <i>R</i> )	sequence
RG201	7	29	79	12	W104C/A281C/A282F
RG202	8	30	83	15	W104C/A281V/A282L
RG204	7	40	74	11	W104C/A281V/A282V
RG301	9	45	90	40	W104C/L144Y/V149I/A281C/A282F
RG302	4	32	87	21	W104C/L144Y/A281C/A282F
RG303	8	39	88	27	W104C/V149D/A281C/A282F
RG305	4	38	87	24	W104C/L144Y/V149D/A281C/A282F
RG308	4	34	88	23	W104C/L144Y/V149H/A281C/A282F
RG309	6	40	86	23	W104C/L144V/V149G/A281V/A282L
RG310	6	34	88	24	W104C/L144F/V149C/A281V/A282L
RG311	6	52	82	29	W104C/L144F/V149G/A281V/A282L
RG313	4	33	86	20	W104C/L144F/V149L/A281C/A282F
RG401	3	49	89	42	W104C/L144Y/V149I/V154I/A281C/A282F

**Table 3. Second and Third Generation S-Selective CALB Mutants as Catalysts in the Kinetic Resolution of *rac*-1**

mutant	reaction time (h)	conversion (%)	ee <sub>S</sub> (%)	<i>E</i> ( <i>S</i> )	sequence
SG201	3,5	49	92	71	I189V/V190C/A281G/A282V
SG202	1	48	84	27	I189V/V190L/A281G/A282V
SG203	12	43	78	15	I189C/V190C/A281G/A282V
SG204	1	49	90	56	V190C/A281G/A282V
SG205	20	18	31	2	I189M/V190W/A281G/A282V
SG206	8	47	50	5	I189V/A281G/A282V
SG301	1	50	91	72	L144Q/I189V/V190C/A281G/A282V
SG302	1	39	91	40	L144R/I189V/V190C/A281G/A282V
SG303	1	45	93	62	V149D/I189V/V190C/A281G/A282V

(Table 4). For example, good to excellent results were observed in the cases of substrates *rac*-4, *rac*-5, *rac*-11, and *rac*-12, with both *R*- and *S*-selectivity being possible in a stereocomplementary manner. Noteworthy are also the reactions of substrates lacking aryl groups in the respective carboxylic acids, for example, *rac*-12 in which the *R*- and *S*-selective mutants are capable of differentiating effectively between ethyl and *n*-butyl substituents at the stereogenic center. When comparing the ethyl ester *rac*-13 with the respective model *p*-nitrophenyl ester *rac*-1 used in the screening process, only *R*-selectivity is accessible. Other limitations were also observed. For example, methyl or isobutyl groups in the *para*-position of the phenyl moiety (*rac*-5, *rac*-6) are tolerated with regard to substrate acceptance, but only moderate enantioselectivity resulted (Table 4, entries 6–14). In the case of more bulky substituents in the *para*-position, unacceptably low activity was observed. In these and other cases, additional mutagenesis

experiments would be necessary. Some evolved mutants showing lower enantioselectivity than the two best hits as catalysts in the reaction of *rac*-1 proved to be superior catalysts in the hydrolysis of the other substrates as well (Tables S1–S6 in the Supporting Information).

#### Enantiocomplementarity in the Hydrolytic Kinetic Resolution of the Acetate of a Chiral Secondary Alcohol.

As already mentioned, the primary application domain of WT CALB involves the stereoselective acylation of chiral secondary alcohols or the hydrolytic reverse reaction, which in numerous cases, hardly needs improvement. Nevertheless, we were interested to see how some of the best mutants evolved for *rac*-1 perform when used as catalysts in the hydrolytic kinetic resolution of acetate *rac*-14 with formation of the *R*- or *S*-alcohol **15**, respectively (Scheme 3).

There was no stringent reason to expect analogous stereocomplementarity for this substrate or in fact any degree of stereoselectivity. We were therefore pleased to discover that some of the CALB mutants which are *S*-selective for *rac*-1 show in the reaction of the acetate *rac*-14 high enantioselectivity, comparable to WT CALB (Table 5). Moreover, reversal of enantioselectivity in favor of the alcohol (*S*)-**15** is possible using mutants that were again evolved for *rac*-1, although only up to an *E* value of 23 (Table 5).

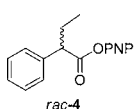
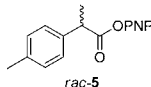
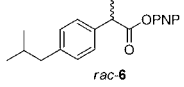
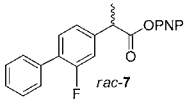
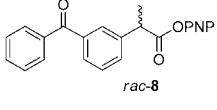
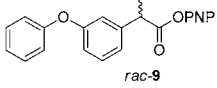
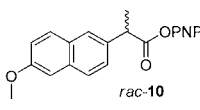
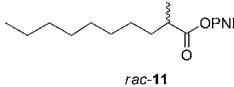
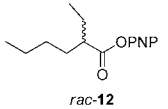
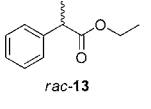
**Kinetic Studies.** Although the UV/visible-based pretest indicated qualitatively that the CALB mutants are more active than the WT, it was important to obtain precise kinetic data. For this purpose, a select group of purified mutants were used as catalysts in the hydrolysis of separately synthesized *R*- and *S*-substrates **1**, **4**, **6**, and **11**, thereby leading to *E* values based on kinetic data that may differ slightly from the values obtained by the Sih equation.<sup>25</sup> The results summarized in Table 6 reveal some remarkable trends. For example, upon going from WT CALB to mutant SG303,  $k_{\text{cat}}/K_{\text{m}}$  increases drastically from 165 to 45 800 M<sup>-1</sup> s<sup>-1</sup>. In the case of *S*-selectivity in reactions of substrates **4**, **6**, and **11**, a similar phenomenon occurs. When aiming for reversal of stereoselectivity in favor of the *R*-configured products, rate enhancement relative to the WT is not as pronounced. Nevertheless, in the case of the model compound (*rac*-1), the *R*-selective mutant (RG401) has a 15-fold higher activity for the *R*-enantiomer and a 2.6-fold lower activity for the *S*-enantiomer relative to WT CALB. Further kinetic studies were performed for substrates **5**, **7**, **8**, **10**, and **12** (see the Supporting Information, Table S8)

**Thermostability of Evolved CALB Mutants.** The introduction of point mutations in an enzyme may lead to a decrease in thermostability.<sup>20,26</sup> While performing the above experiments, we noticed qualitatively that the mutants appear to retain the thermostability characteristic of WT CALB. In order to check quantitatively whether the thermostability of the CALB variants has suffered to any notable degree as a consequence of mutagenesis, the  $T_{50}^{45}$  values were measured for the best mutants, which is the temperature at which 50% residual activity is maintained following a heat treatment of 45 min.<sup>26</sup> The measured  $T_{50}^{45}$  values of WT CALB (56.7 °C) and those of the best mutants SG201 (55 °C) and RG401 (55.2 °C) show that the evolved mutations responsible for enhanced activity and stereoselectivity do not impair the thermostability of the enzyme to any significant degree.

#### Unveiling the Source of Inverted Enantioselectivity.

In order to obtain some insight regarding the source of inverted enantioselectivity induced by the ISM in the stereoselective hydrolysis of *rac*-1, molecular dynamics (MD) simulations and

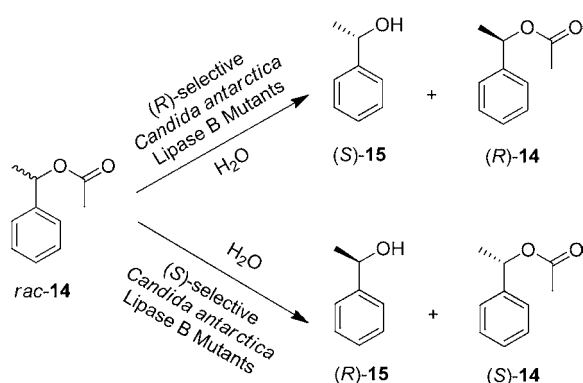
Table 4. Hydrolytic Kinetic Resolution of Different Substrates Using R- and S-Selective CALB Mutants Originally Evolved for *rac-1*

Entry	Substrate	Enzyme	Reaction time (h)	Conv. (%)	ee <sub>p</sub> (S)	<i>E</i> (S) <sup>[a]</sup>	<i>E</i> (R) <sup>[a]</sup>
1	 <i>rac-4</i>	SG301	10	43	88	31	
2		SG204 <sup>[b]</sup>	6,5	44	94	73	
3		WT	16,5	11	4	1	
4		RG401	6,5	41	95		69
5		RG303 <sup>[b]</sup>	4,5	49	93		87
6	 <i>rac-5</i>	SG301	4,5	50	79	20	
7		SG303 <sup>[b]</sup>	4,5	54	83	46	
8		WT	16,5	39	18		2
9		RG401	6,5	45	85		26
10		RG311 <sup>[b]</sup>	6,5	54	83		43
11	 <i>rac-6</i>	SG301	4,5	43	65	8	
12		SG303 <sup>[b]</sup>	6,5	42	75	12	
13		WT	16,5	11	8		1
14		RG401	16,5	39	77		13
15	 <i>rac-7</i>	SG301	3	23	74	9	
16		WT	15	13	8	1	
17		RG401	20	12	59		4
18		RG311 <sup>[b]</sup>	15	22	68		7
19	 <i>rac-8</i>	SG301	5	79	42	11	
20		WT	4	31	21	2	
21		RG401	20	6	33		2
22		RG311 <sup>[b]</sup>	4	34	58		5
23	 <i>rac-9</i>	SG301	0,5	26	84	15	
24		WT	4	25	34	2	
25		RG401	20	16	41		3
26		RG305 <sup>[b]</sup>	15	30	52		5
27	 <i>rac-10</i>	SG301	3	32	67	7	
28		WT	20	9	9	1	
29		RG401	20	19	81		12
30		RG311 <sup>[b]</sup>	15	28	78		11
31	 <i>rac-11</i>	SG301	0,5	47	84	26	
32		SG205 <sup>[b]</sup>	1,5	50	94	115	
33		WT	4	69	24	3	
34		RG401	23	17	66		6
35		RG311 <sup>[b]</sup>	23	24	69		7
36	 <i>rac-12</i>	SG301	1,5	50	>99	>300	
37		WT	23	14	90	21	
38		RG401	23	23	87		19
39		RG101 <sup>[b]</sup>	23	28	93		41
40	 <i>rac-13</i>	SG301	3	41	16	2	
41		WT	3	48	13	1	
42		RG401	6,5	17	93		35
43		RG305 <sup>[b]</sup>	6,5	23	95		50

<sup>a</sup>Mean value of 2–3 reactions. <sup>b</sup>Best mutant for the specified substrate.

docking using GROMACS<sup>27</sup> and Autodock 4.0<sup>28</sup> were performed, respectively, for the evolved mutants SG303 and RG401 that are two of the best variants observed in the present

study. The X-ray crystal structure of CALB lipase (PDB code 1TCA)<sup>8</sup> was utilized as a starting point, and amino acid mutations were introduced using the PyMOL.99rc6 program.<sup>29</sup>

Scheme 3. Stereoselective Hydrolysis of *rac*-14 Catalyzed by CALB MutantsTable 5. Hydrolytic Kinetic Resolution of *rac*-14 with Different R- and S-Selective CALB Mutants Originally Evolved for *rac*-1

mutant	mutation	reaction time (h)	conversion (%)	ee <sub>p</sub> (%)	E (R) <sup>a</sup>	E (S) <sup>a</sup>
WT	—	12	50	>99	>300	
SG303	V149D/V190C/ I189V/A281G/ A282V	12	47	>99	>300	
SG204	V190C/A281G/ A282V	12	30	98	126	
RG105	W104G	11	49	98	>300	
RG104	W104L	11	50	87	40	
RG103	W104M	11	44	56	7	
RG101	W104C	11	44	21		2
RG309	W104C/L144V/ V149G/A281V/ A282L	11	50	81		23
RG310	W104C/L144F/ V149C/A281V/ A282L	11	47	82		22

<sup>a</sup>Mean values are available in the Supporting Information.

First, 4 ns MD simulations were carried out for WT CALB, SG303, and RG401, and their equilibrated conformers were extracted for structure analysis. Remarkable differences in the space dimension of the acyl binding pocket of variants SG303

and RG401 were observed. In mutant SG303, the bottom region of the binding site surrounded by C190, V189, T138, L140, and Q157 (referred to as cavity A) is clearly enlarged relative to the respective space in RG401 and the WT. In Figure 3, the respective distances between the above-mentioned

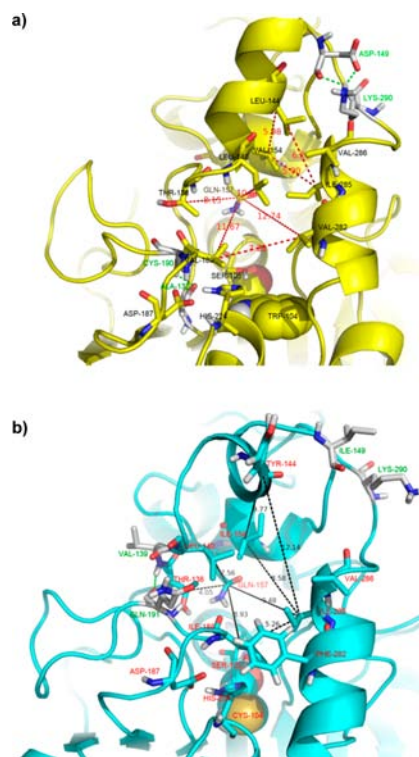


**Figure 3.** (a) Equilibrated conformer of S-selective mutant SG303. (b) Equilibrated conformer of R-selective mutant RG401. Some important residues surrounding the acyl binding sites and catalytic triad (S105-H224-D187) are shown as sticks. Distances defining the dimension of cavity A and crevice B are labeled as red or black dotted lines. Three groups of H bonds indicated by green dotted lines occur between C190 and A132 (SG303), D149 and K290 (SG303), and Q191 and V139 (RG401).

Table 6. Kinetic Data of WT CALB and Different Mutants as Catalyst in the Hydrolysis of Both Enantiomers of Substrates 1, 4, 6, and 11

enzyme	K <sub>m</sub> (mM)	k <sub>cat</sub> (s <sup>-1</sup> )	k <sub>cat</sub> /K <sub>m</sub> (M <sup>-1</sup> s <sup>-1</sup> )	K <sub>m</sub> (mM)	k <sub>cat</sub> (s <sup>-1</sup> )	k <sub>cat</sub> /K <sub>m</sub> (M <sup>-1</sup> s <sup>-1</sup> )	E (R)	E (S)
		(R)-1			(S)-1			
RG401	0.20	1.52	7600	1.78	0.36	200	38	
WT	0.62	0.10	161	5.71	0.94	165		1
SG303	2.06	1.48	718	0.17	7.65	45 800		64
		(R)-4			(S)-4			
RG401	0.12	0.35	2920	0.69	0.03	43	68	
WT	1.81	0.02	10	6.19	0.33	53		5
SG303	2.27	0.04	17	0.37	0.26	702		41
		(R)-6			(S)-6			
RG401	0.05	0.04	800	0.66	0.11	167	5	
WT	0.84	0.05	59	0.57	0.03	59		1
SG303	0.80	0.14	175	0.41	0.81	1980		11
		(R)-11			(S)-11			
RG401	0.08	0.07	875	0.86	0.06	70	13	
WT	0.43	0.12	279	0.46	0.23	500		2
SG303	1.27	1.20	940	0.93	43.81	47 110		50



residues in SG303 are about 2–3 Å larger than those corresponding distances in RG401. This conformational change is induced by the presence of a new H bond involving C190–SH...O=C–A132 in SG303 (Figure 3a), which is different from the existent H bond of Q191–C=O...HN–V139 in RG401 (Figure 3b). Furthermore, mutation I189V in variant SG303 also contributes to the enlargement of the cavity. In contrast, in variant RG401, the H bond of Q191–C=O...HN–V139 induces two effects that lead to the size reduction of cavity A: (1) movement of loop 187–193 closer to loop 136–140; (2) movement of residue I189 closer to helix 280–286. Moreover, mutation A282F also leads to a decrease in the size of cavity A. In variant SG303, a different crevice defined by several residues located at the top of the whole binding site, such as L144, V154, D149, I285, and V286 (referred to as crevice B), is reduced in size. A completely opposite change occurs in the respective crevice of variant RG401. Thus the acyl binding sites in SG303 and RG401 have been reshaped considerably, leading to different binding modes as shown in Figures 4a and S3 (see the Supporting

Information), respectively. In SG303, the large group (phenyl) at the stereogenic center in the acid moiety of substrate **1** binds preferentially in cavity A eventually resulting in *S*-selectivity. In contrast, crevice B in mutant RG401 is comparatively large enabling the accommodation of the phenyl group; this is the ultimate reason for reversed *R*-selectivity. Point mutation W104C also contributes to the reversal of stereoselectivity because the alcohol moiety (*p*-nitrophenyl ester) of substrate (*R*)-**1** would undergo severe steric clash with W104.

Next, the equilibrated conformers of the mutants were used in docking experiments involving substrates (*R*)-**1** and (*S*)-**1**. The energetically favorable poses of substrates (*R*)-**1** and (*S*)-**1** binding to the reshaped active sites of mutants SG303 and RG401 were extracted from the results of applying Autodock 4.0. In the case of the SG303 mutant, the acyl moiety of the favored substrate (*S*)-**1** is readily accommodated in the enlarged cavity surrounded by V189, T138, L140, and Q157; both the large substituent (phenyl group) and the medium-sized substituent (methyl group) fit in a specified manner. All the hydrogen bonds required for catalysis including the normal stabilization of the oxyanion can occur readily (Figure 4b). In sharp contrast, the slow-reacting enantiomer (*R*)-**1** substrate cannot undergo any favorable stabilization of the oxyanion due to steric reasons (Figure 4c). In the *R*-selective mutant RG401, the reduced space of cavity A cannot accept the whole acyl moiety of substrate (*R*)-**1**, which forces the large substituent (phenyl group) to be accommodated in the enlarged crevice B. Compared to the disfavored substrate (*S*)-**1**, enantiomeric (*R*)-**1** in variant RG401 experiences the necessary H bonds for smooth catalysis, and at the same time, the above-mentioned distances for nucleophilic attack are within an appropriate range (Figure S3b,c in the Supporting Information). These findings are in full accord with the results of the kinetic study (Table 6).

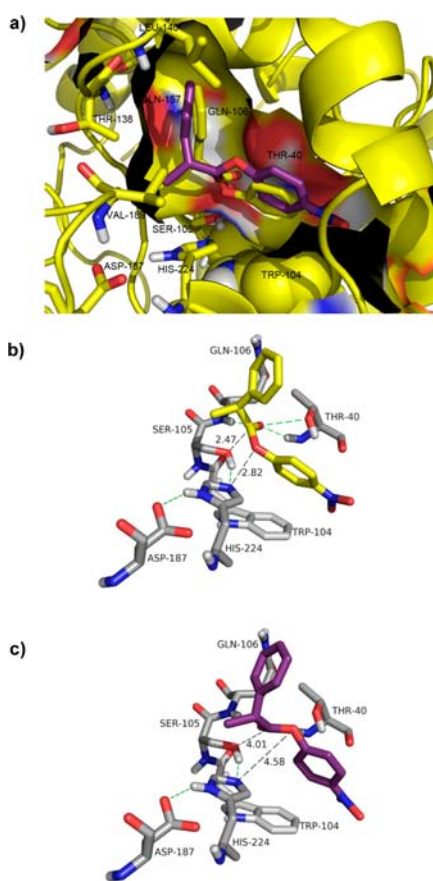


**Figure 4.** (a) Optimized poses of substrates (*S*)-**1** and (*R*)-**1** in *S*-selective mutant SG303. (*S*)-**1** and (*R*)-**1** are shown as yellow and purple sticks, respectively. S105, H224, and D187 define the catalytic triad. (b) Necessary H bonds for catalysis and the stabilization of the oxyanion indicated by green dotted lines occur in the complex of SG303 and (*S*)-**1**; the distances for effective nucleophilic attack of serine in the catalytic triad at the carbonyl function of (*S*)-**1** are labeled as black dotted lines. (c) Oxyanion-stabilizing H bonds in the nonproductive complex of SG303 and (*R*)-**1** are lost, and the distance between catalytically active serine and the carbonyl function is too long.

## CONCLUSIONS

The lipase from *C. antarctica* B (CALB) is one of the most important enzymes in synthetic organic chemistry and biotechnology. It is readily expressed in large quantities and widely used in both academic and industrial applications.<sup>1,2</sup> Although CALB has remarkably high stereoselectivity toward many chiral secondary alcohols and various amines, its ability to catalyze stereoselective reactions of  $\alpha$ -substituted carboxylic acid esters is limited.

Using structure-based saturation mutagenesis in an iterative manner (ISM)<sup>20n,21</sup> coupled with a reduced amino acid alphabet resulting from NDT codon degeneracy,<sup>21,22</sup> we were able to evolve both *R*- and *S*-selective mutants as catalysts for a variety of structurally different  $\alpha$ -chiral esters. Both stereoselectivity and activity were dramatically enhanced. We discovered that targeting randomization sites not only at the acid binding pocket but also at the alcohol binding pocket leads to success. Thus, we conclude, *inter alia*, that the traditional strategy of protein engineers to focus on the alcohol binding site when considering the reaction of chiral alcohols and to focus on the acid binding pocket when working with the esters of chiral carboxylic acids may be successful in some cases, but it diminishes the probability of success. Indeed, long-range effects of point mutations have been reported in other cases.<sup>20</sup> Therefore, we recommend not to adhere to the long-standing practice of dissecting the total binding pocket of a lipase into two separate binding domains.

In the present case, insight regarding the source of stereoselectivity was developed using MD simulations and



docking experiments, especially in the case of inverted enantioselectivity. A reasonable model resulted from these efforts. On the practical side, the enantioselective mutants essentially retained the thermostability of WT CALB. Thus, the range of CALB applications has been expanded considerably.

## ■ ASSOCIATED CONTENT

### ■ Supporting Information

Experimental details including library generation, expression and screening of libraries, enzyme purification and kinetic measurements, kinetic resolution of substrates *rac*-1–14, protocol for upscaling the model reaction using substrate *rac*-1, determination of thermostability, and molecular modeling and MD simulation; all details and data of the hydrolytic kinetic resolution of *rac*-4–14 catalyzed by WT CALB and a series of mutants; kinetic data of WT CALB and mutant-catalyzed hydrolysis of racemic substrates 5, 7, 8, 10, 12; primers used in this work; chiral GC separation conditions; SDS-PAGE of pure WT CALB, RG 401, and SG 303; equilibrated conformer of WT CALB after MD simulation; optimized poses of substrate (*R*)-1 and of (*S*)-1 in *R*-selective mutant RG401. This material is available free of charge via the Internet at <http://pubs.acs.org>.

## ■ AUTHOR INFORMATION

### Corresponding Author

reetz@mpi-muelheim.mpg.de

### Author Contributions

This manuscript was written through contributions of all authors.

### Notes

The authors declare no competing financial interest.

## ■ ACKNOWLEDGMENTS

We thank M. Hermes for the synthesis of all chiral *p*-nitrophenyl esters (1–14) and H. Hinrichs for high-performance liquid chromatography analyses. Q.W. acknowledges the visiting scholarship from “Future Academic Stars” project of Zhejiang University and China Scholarship Council. This work was financed by the Max-Planck-Society.

## ■ REFERENCES

- (1) Reviews of lipases in the production of fine chemicals: (a) Schmid, R. D.; Verger, R. *Angew. Chem., Int. Ed.* **1998**, *37*, 1608–1633. (b) Jaeger, K.-E.; Dijkstra, B. W.; Reetz, M. T. *Annu. Rev. Microbiol.* **1999**, *53*, 315–351. (c) Bornscheuer, U. T.; Kazlauskas, R. J. *Hydrolases in Organic Synthesis: Regio- and Stereoselective Biotransformations*; Wiley-VCH: Weinheim, Germany, 1999. (d) Naik, S.; Basu, A.; Saikia, R.; Madan, B.; Paul, P.; Chatterjee, R.; Brask, J.; Svendsen, A. *J. Mol. Catal. B: Enzym.* **2010**, *65*, 18–23. (e) Sharma, D.; Sharma, B.; Shukla, A. K. *Biotechnology* **2011**, *10*, 23–40. (f) Baldessari, A. *Methods Mol. Biol.* **2012**, *861*, 445–456. (g) Andualema, B.; Gessesse, A. *Biotechnology* **2012**, *11*, 100–118. (h) Houde, A.; Kademi, A.; Leblanc, D. *Appl. Biochem. Biotechnol.* **2004**, *118*, 155–170. (i) Song, X.; Qi, X.; Hao, B.; Qu, Y. *Eur. J. Lipid Sci. Technol.* **2008**, *110*, 1095–1101. (j) Paravidino, M.; Gröger, H.; Hanefeld, U. In *Enzyme Catalysis in Organic Synthesis*; Drauz, K., Gröger, H., May, O., Eds.; Wiley-VCH: Weinheim, Germany, 2012; pp 251–362.
- (2) Kirk, O.; Christensen, M. W. *Org. Prog. Res. Dev.* **2002**, *6*, 446–451.
- (3) Examples of CALB-catalyzed polymerization: (a) Gross, R. A.; Kumar, A.; Kalra, B. *Chem. Rev.* **2001**, *101*, 2097–2124. (b) Kobayashi, S.; Uyama, H.; Kimura, S. *Chem. Rev.* **2001**, *101*, 3793–3818. (c) Takwa, M.; Wittrup Larsen, M.; Hult, K.; Martinelle, M. *Chem. Commun.* **2011**, *47*, 7392–7394. (d) van der Mee, L.; Helmich, F.; de

Bruijn, R.; Vekemans, J. A. J. M.; Palmans, A. R. A.; Meijer, E. W. *Macromolecules* **2006**, *39*, 5021–5027.

(4) (a) Alatorre-Santamaría, S.; Gotor-Fernández, V.; Gotor, V. *Eur. J. Org. Chem.* **2011**, *6*, 1057–1063. (b) Patterson, L. D.; Miller, M. J. *J. Org. Chem.* **2010**, *75*, 1289–1292. (c) Santaniello, E.; Casati, S.; Ciuffreda, P. *Curr. Org. Chem.* **2006**, *10*, 1095–1123.

(5) (a) Pàmies, O.; Bäckvall, J.-E. *Chem. Rev.* **2003**, *103*, 3247–3261. (b) Pàmies, O.; Bäckvall, J.-E. *Trends Biotechnol.* **2004**, *22*, 130–135. (c) Edin, M.; Steinreiber, J.; Bäckvall, J.-E. *Proc. Natl. Acad. Sci. U.S.A.* **2004**, *101*, 5761–5766. (d) Deska, J.; Ochoa, C. D.; Bäckvall, J.-E. *Chem.—Eur. J.* **2010**, *16*, 4447–4451.

(6) (a) Kim, M.-J.; Kim, H. M.; Kim, D.; Ahn, Y.; Park, J. *Green Chem.* **2004**, *6*, 471–474. (b) Kim, M.-J.; Kim, W.-H.; Han, K.; Choi, Y. K.; Park, J. *Org. Lett.* **2007**, *9*, 1157–1159. (c) Ko, S.-B.; Baburaj, B.; Kim, M.-J.; Park, J. *J. Org. Chem.* **2007**, *72*, 6860–6864.

(7) Promiscuous reactions catalyzed by CALB: (a) Branneby, C.; Carlqvist, P.; Hult, K.; Brinck, T.; Berglund, P. *J. Mol. Catal. B: Enzym.* **2004**, *31*, 123–128. (b) Branneby, C.; Carlqvist, P.; Magnusson, A.; Hult, K.; Brinck, T.; Berglund, P. *J. Am. Chem. Soc.* **2003**, *125*, 874–875. (c) Carlqvist, P.; Svedendahl, M.; Branneby, C.; Hult, K.; Brinck, T.; Berglund, P. *ChemBioChem* **2005**, *6*, 331–336. (d) Svedendahl, M.; Hult, K.; Berglund, P. *J. Am. Chem. Soc.* **2005**, *127*, 17988–17989. (e) Carlqvist, P.; Eklund, R.; Hult, K.; Brinck, T. *J. Mol. Model.* **2003**, *9*, 164–171. (f) Carboni-Oerlemans, C.; Domínguez de María, P.; Tuin, B.; Bargeman, G.; van der Meer, A.; van Gemert, R. *J. Biotechnol.* **2006**, *126*, 140–151. (g) Rustoy, E. M.; Sato, Y.; Nonami, H.; Erra-Balsells, R.; Baldessari, A. *Polymer* **2007**, *48*, 1517–1525. (h) Sharma, U. K.; Sharma, N.; Kumar, R.; Kumar, R.; Sinha, A. K. *Org. Lett.* **2009**, *11*, 4846–4848. (i) Wu, Q.; Liu, B.-K.; Lin, X.-F. *Curr. Org. Chem.* **2010**, *14*, 1966–1988.

(8) (a) Uppenberg, J.; Hansen, M. T.; Patkar, S.; Jones, T. A. *Structure* **1994**, *2*, 293–308. (b) Uppenberg, J.; Oehrner, N.; Norin, M.; Hult, K.; Kleywegt, G. J.; Patkar, S.; Waagen, V.; Anthonen, T.; Jones, T. A. *Biochemistry* **1995**, *34*, 16838–16851. (c) Otto, R. T.; Scheib, H.; Bornscheuer, U. T.; Pleiss, J.; Sylđat, C.; Schmid, R. D. *J. Mol. Catal. B: Enzym.* **2000**, *8*, 201–211.

(9) Kazlauskas, R. J.; Weissfloch, A. N. E.; Rappaport, A. T.; Cuccia, L. A. *J. Org. Chem.* **1991**, *56*, 2656–2665.

(10) Kirk, O.; Björkling, F.; Godtfredsen, S.; Ostfeld Larsen, T. *Biocatal. Biotransform.* **1992**, *6*, 127–134.

(11) (a) Arroyo, M.; Sinisterra, J. V. *J. Org. Chem.* **1994**, *59*, 4410–4417. (b) Hollmann, F.; Grzebyk, P.; Heinrichs, V.; Doderer, K.; Thum, O. *J. Mol. Catal. B: Enzym.* **2009**, *57*, 257–261. (c) Klomp, D.; Peters, J. A.; Hanefeld, U. *Tetrahedron: Asymmetry* **2005**, *16*, 3892–3896. (d) Ong, A. L.; Kamaruddin, A. H.; Bhatia, S.; Aboul-Enein, H. Y. *J. Sep. Sci.* **2008**, *31*, 2476–2485. (e) Wang, P.-Y.; Chen, Y.-J.; Wu, A.-C.; Lin, Y.-S.; Kao, M.-F.; Chen, J.-R.; Ciou, J.-F.; Tsai, S.-W. *Adv. Synth. Catal.* **2009**, *351*, 2333–2341. (f) Morrone, R.; D’Antona, N.; Lambusta, D.; Nicolosi, G. *J. Mol. Catal. B: Enzym.* **2010**, *65*, 49–51. (g) Juhl, P. B.; Doderer, K.; Hollmann, F.; Thum, O.; Pleiss, J. *J. Biotechnol.* **2010**, *150*, 474–480.

(12) (a) Evans, A. M. *Eur. J. Clin. Pharmacol.* **1992**, *42*, 237–256. (b) Davies, N. M. *Clin. Pharmacokinet.* **1998**, *34*, 101–154.

(13) (a) Shiina, I.; Nakata, K.; Ono, K.; Onda, Y.; Itagaki, M. *J. Am. Chem. Soc.* **2010**, *132*, 11629–11641. (b) Yang, X.; Birman, V. B. *Chem.—Eur. J.* **2011**, *17*, 11296–11304.

(14) (a) Patkar, S.; Vind, J.; Kelstrup, E.; Christensen, M. W.; Svendsen, A.; Borch, K.; Kirk, O. *Chem. Phys. Lipids* **1998**, *93*, 95–101. (b) Zhang, N. Y.; Suen, W.-C.; Windsor, W.; Xiao, L.; Madison, V.; Zaks, A. *Protein Eng., Des. Sel.* **2003**, *16*, 599–605. (c) Patkar, S.; Svendsen, A.; Kirk, O.; Clausen, I. G.; Borch, K. *J. Mol. Catal. B: Enzym.* **1997**, *3*, 51–54. (d) Chodorge, M.; Fourage, L.; Ullmann, C.; Duvivier, V.; Masson, J.-M.; Lefèvre, F. *Adv. Synth. Catal.* **2005**, *347*, 1022–1026. (e) Costa, L.; Brissos, V.; Lemos, F.; Ramôa Ribeiro, F.; Cabral, J. M. S. *Bioprocess Biosyst. Eng.* **2009**, *32*, 53–61. (f) Suen, W.-C.; Zhang, N.; Xiao, L.; Madison, V.; Zaks, A. *Protein Eng., Des. Sel.* **2004**, *17*, 133–140.

(15) (a) Qian, Z.; Fields, C. J.; Lutz, S. *ChemBioChem* **2007**, *8*, 1989–1996. (b) Qian, Z.; Horton, J. R.; Cheng, X. D.; Lutz, S. *J. Mol.*

- Biol.* **2009**, *393*, 191–201. (c) Qian, Z.; Lutz, S. *J. Am. Chem. Soc.* **2005**, *127*, 13466–13467. (d) Syrén, P.-O.; Lindgren, E.; Hoeffken, H. W.; Branneby, C.; Maurer, S.; Hauer, B.; Hult, K. *J. Mol. Catal. B: Enzym.* **2010**, *65*, 3–10. (e) Liu, D.; Trodler, P.; Eiben, S.; Koschorreck, K.; Müller, M.; Pleiss, J.; Maurer, S. C.; Branneby, C.; Schmid, R. D.; Hauer, B. *ChemBioChem* **2010**, *11*, 789–795. (f) Wittrup Larsen, M.; Zielinska, D. F.; Martinelle, M.; Hidalgo, A.; Juhl Jensen, L.; Bornscheuer, U. T.; Hult, K. *ChemBioChem* **2010**, *11*, 796–801.
- (16) (a) Jung, S.; Park, S. *Biotechnol. Lett.* **2008**, *30*, 717–722. (b) Budisa, N.; Wenger, W.; Wiltschi, B. *Mol. BioSyst.* **2010**, *6*, 1630–1639. (c) Wittrup Larsen, M.; Bornscheuer, U. T.; Hult, K. *Protein Expression Purif.* **2008**, *62*, 90–97. (d) Kim, S. Y.; Sohn, J. H.; Pyun, Y. R.; Yang, I. S.; Kim, K. H.; Choi, E. S. *J. Microbiol. Biotechnol.* **2007**, *17*, 1308–1315.
- (17) (a) Rotticci, D.; Rotticci-Mulder, J. C.; Denman, S.; Norin, T.; Hult, K. *ChemBioChem* **2001**, *2*, 766–770. (b) Magnusson, A. O.; Hult, K.; Holmquist, M. *J. Am. Chem. Soc.* **2001**, *123*, 4354–4355. (c) Magnusson, A. O.; Rotticci-Mulder, J. C.; Santagostino, A.; Hult, K. *ChemBioChem* **2005**, *6*, 1051–1056. (d) Magnusson, A. O.; Takwa, M.; Hamberg, A.; Hult, K. *Angew. Chem., Int. Ed.* **2005**, *44*, 4582–4585. (e) Vallin, M.; Syrén, P.-O.; Hult, K. *ChemBioChem* **2010**, *11*, 411–416. (f) Engström, K.; Vallin, M.; Syrén, P. O.; Hult, K.; Bäckvall, J. E. *Org. Biomol. Chem.* **2011**, *9*, 81–82. (g) Marton, Z.; Léonard-Nevers, V.; Syrén, P.-O.; Bauer, C.; Lamare, S.; Hult, K.; Tranc, V.; Graber, M. *J. Mol. Catal. B: Enzym.* **2010**, *65*, 11–17. (h) Svendsen, A. *Biochim. Biophys. Acta* **2000**, *1543*, 223–238.
- (18) Skjöt, M.; De Maria, L.; Chatterjee, R.; Svendsen, A.; Patkar, S. A.; Østergaard, P. R.; Brask, J. *ChemBioChem* **2009**, *10*, 520–527.
- (19) (a) Engström, K.; Nyhlén, J.; Sandström, A. G.; Bäckvall, J.-E. *J. Am. Chem. Soc.* **2010**, *132*, 7038–7042. (b) Sandström, A. G.; Wikmark, Y.; Engström, K.; Nyhlén, J.; Bäckvall, J.-E. *Proc. Natl. Acad. Sci. U.S.A.* **2012**, *109*, 78–83.
- (20) Recent reviews of directed evolution: (a) Lutz, S.; Bornscheuer, U. T. *Protein Engineering Handbook*; Wiley-VCH: Weinheim, Germany, 2009; Vol. 1–2. (b) Quin, M. B.; Schmidt-Dannert, C. *ACS Catal.* **2011**, *1*, 1017–1021. (c) Turner, N. J. *Nat. Chem. Biol.* **2009**, *5*, 567–573. (d) Bommarius, A. S.; Blum, J. K.; Abrahamson, M. *J. Curr. Opin. Chem. Biol.* **2011**, *15*, 194–200. (e) Dalby, P. A. *Curr. Opin. Struct. Biol.* **2011**, *21*, 473–480. (f) Jäckel, C.; Hilvert, D. *Curr. Opin. Biotechnol.* **2010**, *21*, 753–759. (g) Brustad, E. M.; Arnold, F. H. *Curr. Opin. Chem. Biol.* **2011**, *15*, 201–210. (h) Bershtein, S.; Tawfik, S. *Curr. Opin. Chem. Biol.* **2008**, *12*, 151–158. (i) Shivange, A. V.; Marienhagen, J.; Mundhada, H.; Schenk, A.; Schwaneberg, U. *Curr. Opin. Chem. Biol.* **2009**, *13*, 19–25. (j) Kumar, A.; Singh, S. *Crit. Rev. Biotechnol.* **2012**, DOI: 10.3109/07388551.2012.716810. (k) Siloto, R. M. P.; Weselake, R. J. *Biocatal. Agric. Biotechnol.* **2012**, *1*, 181–189. (l) Bolt, A.; Berry, A.; Nelson, A. *Arch. Biochem. Biophys.* **2008**, *474*, 318–330. (m) Wang, M.; Si, T.; Zhao, H. *Bioresour. Technol.* **2012**, *115*, 117–125. (n) Reetz, M. T. *Tetrahedron* **2012**, *68*, 7530–7548.
- (21) Review of directed evolution of stereoselective enzymes<sup>20n</sup> with emphasis on iterative saturation mutagenesis: Reetz, M. T. *Angew. Chem., Int. Ed.* **2011**, *50*, 138–174.
- (22) Reetz, M. T.; Carballeira, J. D. *Nat. Protoc.* **2007**, *2*, 891–903.
- (23) Reetz, M. T.; Zonta, A.; Schimossek, K.; Liebeton, K.; Jaeger, K.-E. *Angew. Chem., Int. Ed. Engl.* **1997**, *36*, 2830–2832.
- (24) Gumulya, Y.; Sanchis, J.; Reetz, M. T. *ChemBioChem* **2012**, *13*, 1060–1066.
- (25) Chen, C.-S.; Fujimoto, Y.; Girdaukus, G.; Sih, C. J. *J. Am. Chem. Soc.* **1982**, *104*, 7294–7299.
- (26) Reviews of protein engineering of thermostability:<sup>22</sup>  
(a) O’Fagain, C. *Enzyme Microb. Technol.* **2003**, *33*, 137–149.  
(b) Eijsink, V. G. H.; Gåseidness, S.; Borchert, T. V.; van den Burg, B. *Biomol. Eng.* **2005**, *22*, 21–30. (c) Wintrode, P. L.; Arnold, F. H. *Adv. Protein Chem.* **2001**, *55*, 161–225.
- (27) (a) Berendsen, H. J. C.; van der Spoel, D.; van Drunen, R. *Comput. Phys. Commun.* **1995**, *91*, 43–56. (b) van der Spoel, D.; Lindahl, E.; Hess, B.; Groenhof, G.; Mark, A. E.; Berendsen, H. J. C. *J. Comput. Chem.* **2005**, *26*, 1701–1718.
- (28) Morris, G. M.; Goodsell, D. S.; Halliday, R. S.; Huey, R.; Hart, W. E.; Belew, R. K.; Olson, A. J. *J. Comput. Chem.* **1998**, *19*, 1639–1662.
- (29) DeLano, W. L. *The PyMOL Molecular Graphics System*; DeLano Scientific: San Carlos, CA, 2002; <http://www.pymol.org>.